Formation and sintering of $(Y_{1-x}Ce_x)MnO_3$ ($0 \leq x \leq 0.06$) via a citric acid process

K. HIROTA*, K. FUJITA, M. YOSHINAKA, O. YAMAGUCHI
Department of Molecular Science and Technology, Faculty of Engineering, Doshisha University, Kyo-Tanabe, Kyoto 610-0321, Japan
E-mail: khirota@mail.doshisha.ac.jp

Hexagonal ABO_3 compounds have basically different structure from perovskite ABO_3 compounds. Among these, non-perovskite $AMnO_3$ has attracted much interest due to the coexistence of ferroelectric and ferromagnetic behavior [1].

In the present study, the effect of Ce addition to hexagonal $YMnO_3$ was investigated from the viewpoint of formation of solid solutions and fabrication of dense ceramics using fine powders prepared by a citric acid process [2]. Till now, little information has been available on the effects of Ce-addition and the fabrication of dense $YMnO_3$ ceramics without micro-cracks. This might be due to a phase transition from orthorhombic to hexagonal at 960 °C accompanied by a ≈10% volume change [3].

Reagent-grade $Y(NO_3)_3{\cdot}6H_2O$, $Mn(NO_3)_2{\cdot}6H_2O$, and $Ce(NO_3)_3{\cdot}6H_2O$ and anhydrous citric acid (CA) were used as starting materials. Table I shows the nominal compositions of the samples. Yttrium, manganese, and cerium nitrates corresponding to each composition were dissolved into 0.5 L distilled water; their concentration was 2 mol/L. A large amount of aqueous solution containing CA was added to the mixed-metal solutions at room temperature. Then the mixed solutions were heated at 100 °C for 5 hr and stirred to the gelatinous state. The obtained gel products (precursors) were dried. Pulverized precursors were slowly heated in air to 500 °C and then held for 2 hr to burn out the organic substances. As-prepared precursors A through F (Table I) were amorphous to X-ray. A differential thermal analysis (DTA) curve of precursor A revealed a high broad exothermic peak resulting from a combustion of CA at approximately 220–300 °C. No significant change in structure was observed until 830 °C. Small exothermic and endothermic peaks were detected at 830–850 °C and 1200–1220 °C, respectively. X-ray diffraction (XRD) analysis using $CuK_{\alpha 1}$ radiation equipped with a monochromator revealed that orthorhombic(o) $YMnO_3$ [4] phase began to appear in precursor A when heated to 850 °C and became stronger at 900 °C, suggesting that the exothermic peak correspond to the crystallization of o-$YMnO_3$. In addition, precursors B through E showed hexagonal (h) $YMnO_3$ phase [5]. XRD line intensities of the latter phase increased with increasing Ce content and finally the former phase diminished at $x = 0.10$. From this, it is possible to state that a small amount of Ce addition stabilizes the high-temperature phase. From XRD analysis, it was clear that Samples A to D heated above 1200 °C consisted of only h-$YMnO_3$, whereas, E and F were a mixture of h-$YMnO_3$, CeO_2 [6], and Mn_3O_4 [7]. These results indicate that the endothermic peaks corresponded to the orthorhombic-hexagonal $YMnO_3$ phase transition. However, after calcination at 1100 °C for 2 hr, even below the endothermic peak temperature, all the samples, except for E and F revealed h-$YMnO_3$ phase. Fig. 1 shows TEM photographs of these calcined powders; it should be noted that particles of pure $YMnO_3$ were much larger than those of Ce-doped $YMnO_3$. In addition the particles of the latter increased in size from approximately 0.10–0.30 μm and tended to be aggregated with increasing Ce content. Fig. 2 shows the lattice parameters (a and c) for h-$YMnO_3$ phase obtained at 1500 °C. All the samples from A through F consisted of only h-$YMnO_3$ phase. The values of a and c were determined by a least-squares refinement with an internal standard of high-purity Si. Pure h-$YMnO_3$ exhibited parameters of $a = 0.6145(2)$ and

TABLE I Nominal compositions and some characteristics of $(Y_{1-x}Ce_x)MnO_3$ ($0 \leq x \leq 0.06$) solid solution ceramics sintered for 4 hr at 1500 °C in air

Theoretical density ($Mg{\cdot}m^{-3}$)	Bulk density ($Mg{\cdot}m^3$)	Relative density (%)	Average grain size G_s(μ m)	Electrical conductivity σ at 1273 K $S{\cdot}m^{-1}$	Activation energy E_a(eV)
5.128	4.98	97.1	4.9	3.9×10^0	1.21(at high temperatures)
5.157	5.00	97.1	5.6	2.4×10^1	1.16
5.176	5.03	97.2	7.0	4.4×10^1	1.14
5.197	5.06	97.3	8.3	5.7×10^1	1.09
–	–	–	–	–	–
–	–	–	–	–	–

*Author to whom all correspondence should be addressed.

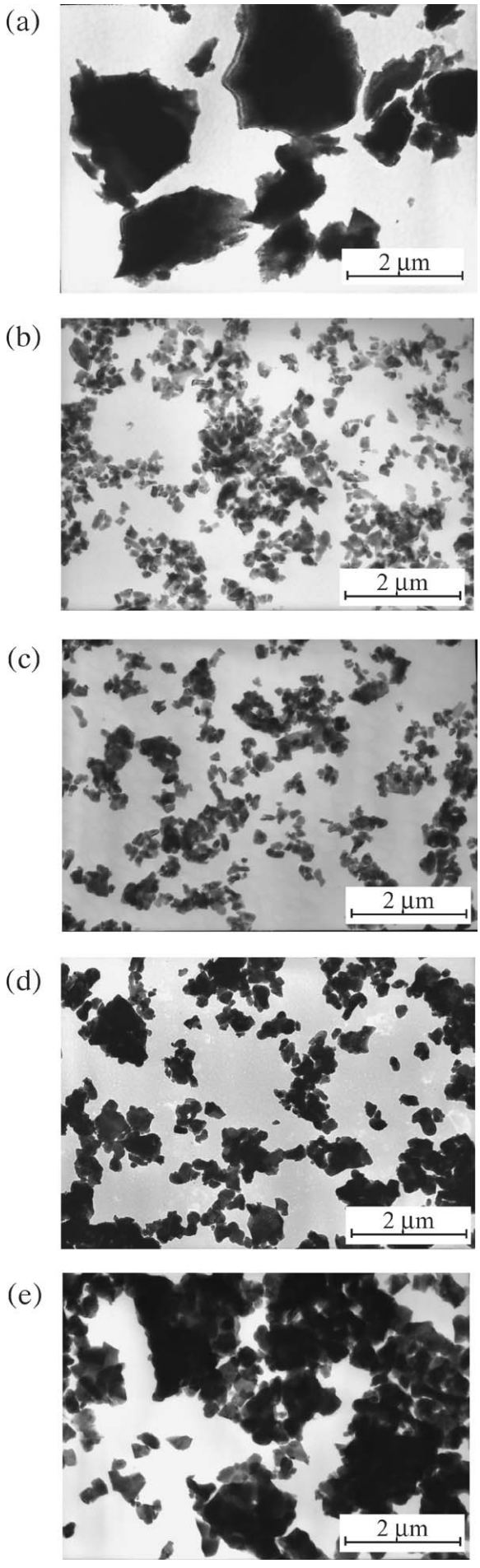

Figure 1 TEM photographs of hexagonal $(Y_{1-x}Ce_x)MnO_3$ powders prepared by heating for 2 hr at 1100 °C: (a) $x = 0.0$, (b) $x = 0.02$, (c) $x = 0.04$, (d) $x = 0.06$, and (e) $x = 0.08$.

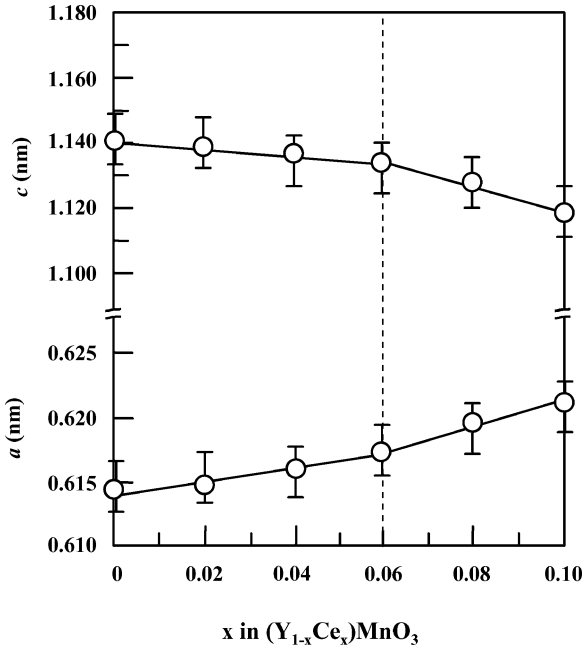

Figure 2 Lattice parameters (a and c) of hexagonal $YMnO_3$ phase prepared by heating for 4 hr at 1500 °C as a function of Ce content.

$c = 1.1403(4)$ nm, agreeing with those ($a = 0.61360$ and $c = 1.1400$ nm) reported for h-$YMnO_{2.93}$ [5]. As shown in Fig. 2, with increasing x, the values of a increased whilst those of c decreased linearly from 0.6145(2) to 0.6172(3) and from 1.1403(4) to 1.1320(4) nm respectively up to $x = 0.06$, with the slopes becoming a little steeper above this point. In the $YMnO_3$ structure, the co-ordination number of the A-site cation is nine [8] and the ionic radii of Y^{3+} and Ce^{4+} are 0.1075 and −0.1015 nm, respectively [9]. Therefore a decrease in the parameter c could be explained in terms of the replacement of large Y^{3+} with small Ce^{4+}. On the other hand, Ce-addition introduces Mn^{2+} into the $YMnO_3$ structure: $(Y^{3+}_{1-x}\ Ce^{4+}_{x})[Mn^{3+}_{1-x}\ Mn^{2+}_{x}]O_3$. The radii of the six-fold B-site [8] Mn^{2+} and Mn^{3+} are 0.0830 and 0.0645 nm, respectively [9]. Therefore, an increase in parameter a might originate from an increasing amount of larger Mn^{2+}. The behavior shown in Fig. 2, although different from the normal compositional dependence of lattice parameters in solid solutions, was also reported for Zr-doped h-$YMnO_3$ [$Y_{1-x}\ Zr_xMnO_3$] [10]. Aken *et al.* [10] explained that this lattice parameter change might be due to the shift of Zr^{4+} distribution from 100% A-site to A/B mixed sites. From these results, it might be said that the same phenomenon could also occur in Ce-doped h-$YMnO_3$. Thus, h-$YMnO_3$ solid solutions containing up to −6 mol% Ce could be formed via a citric acid process.

The $(Y_{1-x}Ce_x)MnO_3$ ($0 \leq x \leq 0.06$) powders were sintered as follows. After calcination (1100 °C for 2 hr), well-pulverized powders with a small amount of water were uniaxially (70 MPa) and isostatically (295 MPa) pressed into disks. Powder compact thus obtained were 16 mm in diameter and 5 mm high. They were covered by powders with the same composition and heated in air. Sintering was performed at 1110 and 1250 °C each for 2 hr, and at 1500 °C for 4 hr with heating rates of 600 °C/hr (room temperature to 1100 °C)

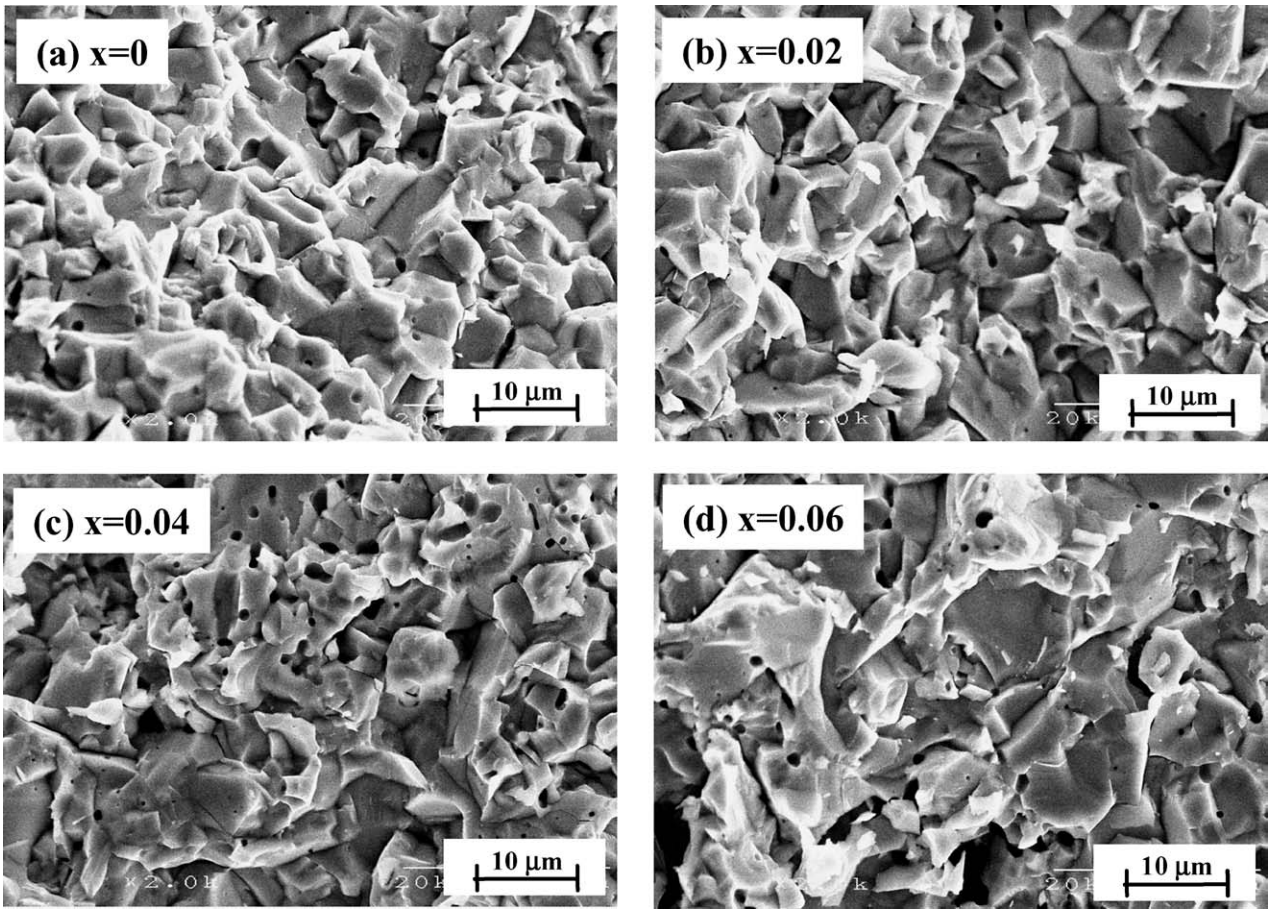

Figure 3 SEM micrographs of fracture surfaces of $(Y_{1-x}Ce_x)MnO_3$ ceramics sintered for 4 hr at 1500 °C in air: (a) $x = 0$, (b) $x = 0.02$, (c) $x = 0.04$, and (d) $x = 0.06$.

and 300 °C/hr (1100–1500 °C). Samples were cooled at a rate of 300 °C/hr from 1500–1100 °C, followed by furnace-cooling.

Sintered compacts consisted of only h-$YMnO_3$ phase. Their bulk densities, measured by the Archimedes method, increased from 4.98 to 5.06 Mg·m^{-3} with increasing Ce content, corresponding to 97.1–97.3% of theoretical density (Table I). Relative densities increased gradually with increase in x. Fig. 3 shows scanning electron microscope (SEM) micrographs of fracture surfaces with homogeneous microstructures consisting of equi-axial grains from 4.9 to 8.3 μm in size. From these, it appears that Ce addition enhanced grain growth a little during sintering. Micro-cracks, previously reported as being present on the free surfaces of h-$YMnO_3$ ceramics sintered for 2 hr at 1500 °C [3], were not detected. This might be explained in terms of a moderate sintering condition, no phase transformation, and a Ce-stabilizing effect.

D.C. electrical conductivity σ was measured at 673–1273 K by a four-probe technique. Qualitative Seebeck measurement for these ceramics shows that they exhibit p-type behavior. Fig. 4 shows the temperature dependence of σ in a plot of $\log_{10}(\sigma T)$ against reciprocal absolute temperature (T). It should be noted that only pure $YMnO_3$ showed an inflexion around 700 °C, although, other solid solution ceramics exhibit straight lines. According to these results, it would be said that the electrical conductivity mechanism is based on thermally activated hopping of small polarons

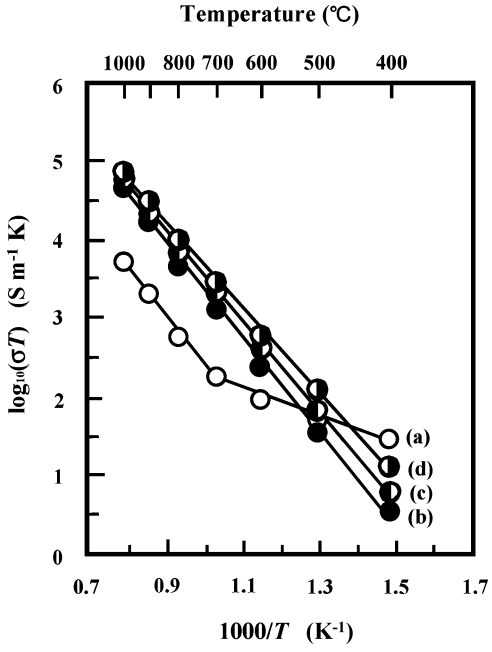

Figure 4 $\log_{10}(\sigma T)$ vs. $1000/T$ for $(Y_{1-x}Ce_x)MnO_3$ ceramics: (a) $x = 0$, (b) $x = 0.02$, (c) $x = 0.04$, and (d) $x = 0.06$.

between localized states corresponding to B-site of different valence, Mn^{2+}–Mn^{3+} [10], as supported by the conduction mechanism for $ReMnO_3$ [11]. Till now, a little attention has been given to the electrical properties of pure $YMnO_3$, only σ measured at room temperature to −250 °C have been reported [12].

In the present study, σ of h-$YMnO_3$ solid solution ceramics without micro-cracks has been measured at high temperatures. The value of σ at 1273 K increases ($3.9 \times 10^{\circ} \rightarrow 5.7 \times 10^{1}$ $S \cdot m^{-1}$) and the activation energy E_a at high temperatures decreases ($1.21 \rightarrow 1.09$ eV) with increased Ce content.

Acknowledgments

This work was supported by a grant to Research Center for Advanced Science and Technology at Doshisha University from the Ministry of Education, Science, Sports and Culture, Japan.

References

1. N. A. HILL, *J. Phys. Chem.* **B104** (2000) 6694.
2. M. P. PECHINI, U.S. Patent No. 3 330 697 (July 1967).
3. B. FU and W. HUEBNER, *J. Mater. Res.* **9** (1994) 2645.
4. Powder Diffraction File, Card No. 20-732. Joint Committee on Powder Diffraction Standards, Swarthmore PA, 1979.
5. *Ibid.*, Card No. 25-1079, 1984.
6. *Ibid.*, Card No. 34-394, 1989.
7. *Ibid.*, Card No. 13-162, 1972.
8. B. B. VAN AKEN, A. MEETSMA and T. T. M. PALSTRA, *Acta Crystallogr. Sect. C: Cryst. Struct. Commun.* **57** (2001) 230.
9. R. D. SHANNON and C. T. PREWITT, *J. Inorg. Nucl. Chem.* **30** (1968) 1389.
10. B. B. VAN AKEN, J.-W. G. BOS, R. A. DE GROOT and T. T. M. PALSTRA, *Phys. Rev.* **B63** (2001) 125127.
11. L. BALCELLS, R. ENRICH, J. MORA, A. CALLEJA, J. FONTCUBERTA and X. OBRADORS, *Appl. Phys. Lett.* **69** (1996) 1486.
12. C. MOURE, M. VILLEGAS, J. F. FERNANDEZ, J. TARTAJ and P. DURAN, *J. Mater. Sci.* **34** (1999) 2565.

Received 9 October 2003
and accepted 23 June 2004